


RESEARCH ARTICLE

Effects of ceramic additives and bioactive coatings on the degradation of polylactic acid-based bone scaffolds under hydrolytic conditions

Ricardo Donate¹  | Mario Monzón¹ | María Elena Alemán-Domínguez¹ | Francisco Rodríguez-Esparragón²

¹Departamento de Ingeniería Mecánica, Grupo de Investigación en Fabricación Integrada y Avanzada, Universidad de Las Palmas de Gran Canaria, Las Palmas, Spain

²Unidad de Investigación, Hospital Universitario de Gran Canaria Doctor Negrín, Las Palmas, Spain

Correspondence

Ricardo Donate, Departamento de Ingeniería Mecánica, Grupo de Investigación en Fabricación Integrada y Avanzada, Universidad de Las Palmas de Gran Canaria, Campus Universitario de Tafira s/n, 35017 Las Palmas, Spain.

Email: ricardo.donate@ulpgc.es

Funding information

Agencia Canaria de Investigación, Innovación y Sociedad de la Información, Grant/Award Number: TESIS2017010036; Ministerio de Ciencia e Innovación, Grant/Award Number: UNLP10-3E-726; Ministerio de Ciencia, Innovación y Universidades, Grant/Award Number: DPI2017-88465-R; European Social Fund (ESF)

Abstract

Poly(lactic acid) (PLA) has been extensively used for the manufacturing of scaffolds in bone tissue engineering applications. Due to the low hydrophilicity and the acidic degradation process of this biomaterial, different strategies have been proposed to increase the biofunctionality of the support structure. The use of ceramic particles is a generally preferred option to increase the osteoconductivity of the base material, while acting as buffers to maintain the pH level of the surrounding tissues. Surface modification is another approach to overcome the limitations of PLA for tissue engineering applications. In this work, the degradation profile of 3D-printed PLA scaffolds containing beta-tricalcium phosphate (β -TCP) and calcium carbonate (CaCO_3) particles has been studied under hydrolytic conditions. Composite samples treated with plasma and coated with Aloe vera extracts were also studied to evaluate the effect of this surface modification method. The characterization of the 3D structures included its morphological, calorimetric and mechanical evaluation. According to the results obtained, the proposed composite scaffolds allowed an adequate maintenance of the pH level of the surrounding medium, with no effects observed on the morphology and mechanical properties of these structures. Hence, these samples showed potential to be further investigated as candidates for bone tissue regeneration.

KEYWORDS

additive manufacturing, bioceramics, biomaterials, bone tissue engineering, surface coating

1 | INTRODUCTION

As a bioresorbable and biodegradable polymer, polylactic acid (PLA) is one of the most promising and extensively investigated biomaterials for scaffold manufacturing in the bone tissue engineering (BTE) field, mainly due to its biocompatibility, suitable mechanical properties for load-bearing applications, good processability by additive manufacturing

(AM) techniques and adjustable degradation rate.¹⁻³ However, some of the limitations imposed by PLA include^{2,4}: (a) its brittleness; (b) low hydrophilicity, which results in low cell-material interaction; (c) slow degradation rate; (d) lack of reactive side-chain groups; and (e) inflammatory reactions in vivo due to the release of acidic degradation byproducts.

The methyl group in the backbone of the polymer has an effect on both the hydrophobicity of the material and the resistance of the

This is an open access article under the terms of the [Creative Commons Attribution-NonCommercial-NoDerivs](https://creativecommons.org/licenses/by-nc-nd/4.0/) License, which permits use and distribution in any medium, provided the original work is properly cited, the use is non-commercial and no modifications or adaptations are made.

© 2022 The Authors. *Journal of Biomedical Materials Research Part B: Applied Biomaterials* published by Wiley Periodicals LLC.

structure to hydrolytic degradation.^{1,5} The degradation rate of PLA-based scaffolds depends on their crystallinity, molecular weight and its distribution, morphology, the water diffusion rate into the polymer and the stereoisomeric content.⁶ By tuning these properties, the degradation rate of PLA-based scaffold can be adjusted to match that of bone tissue regeneration, while providing sufficient mechanical support and without causing any adverse response on the surrounding tissues⁷ before being excreted through metabolic pathways. Despite these modifications, PLA would still lack on surface epitopes that could promote osteoconductivity and cell affinity.³

To overcome these drawbacks, different strategies have been proposed in the literature to enhance surface biofunctionalization. The most common one is the addition into the PLA matrix of bioactive ceramic particles that can act as buffers to counteract the acidic degradation byproducts, modulate the degradation rate, increase the osteoconductivity and mechanical properties, and promote cell adhesion and proliferation.¹ Because of their suitable properties (similar composition with natural bone, osteoinductivity, osteoconductivity, biodegradability, and high mechanical strength), hydroxyapatite (HAp)⁸⁻¹⁰ and beta-tricalcium phosphate (β -TCP)¹¹⁻¹³ are the preferred options among the different bioceramic additives studied for BTE applications.

Other strategies to modify the base material properties aiming for bone regeneration applications include plasma treatment,¹⁴ protein adsorption,¹⁵ immobilization of hydrophilic molecules¹⁶ and surface functionalization with bioactive epitopes.¹⁷ However, few studies can be found in the literature regarding the evaluation of composite PLA-based scaffolds coated with biological substances for tissue engineering applications.¹⁸⁻²² The combination of the latter strategies would allow obtaining a functionalized 3D structure both on its surface and at the bulk. Hence, in this work the use of additives and the application of surface modifications were simultaneously used to improve the properties of 3D-printed PLA-based scaffolds. Specifically, calcium carbonate (CaCO_3) and β -TCP were introduced as additives into the polymeric matrix. As demonstrated in our previous study,¹³ the combination of these additives enhances the hydrophilicity and surface roughness of the scaffolds, leading to a significant improvement of the metabolic activity of osteoblastic cells after 7 days of culture. In the present study, PLA and composite scaffolds manufactured by AM were later treated with oxygen plasma and coated with Aloe vera extracts, aiming to attach bioactive compounds that could favor cell adhesion and proliferation. A preliminary biological evaluation of this surface modification method was carried out in a previous work.²³ The *in vitro* cell culture of osteoblastic cells on PLA scaffolds revealed an improvement of cell metabolic activity for Aloe vera coated samples.

The biomedical applications of Aloe vera have been gaining attention recently, since acetylated polysaccharides, the major constituents of Aloe vera inner gels, have been reported to possess antitumor and immunomodulatory activities.²⁴⁻²⁶ Acemannan, a mannose-containing polysaccharide and the main bioactive component of Aloe vera, has also proven to induce bone formation and regeneration.^{27,28} While there are several examples in the literature related to the

incorporation of Aloe vera in the formulation of scaffolds intended for skin regeneration,²⁹⁻³¹ the number of studies comprising the application of Aloe vera coatings in the BTE field remains limited.³²⁻³⁴ Noteworthy, to the best of our knowledge, our previous study²³ is the only work in which an Aloe vera coating was applied to bone scaffolds obtained by AM.

Despite of the extensive literature on strategies to improve the properties of PLA-based scaffolds for BTE applications, little attention has been paid to the effect of such modifications on the degradation profile of the structures. Aiming to evaluate the developed PLA-based scaffolds in a situation close to the clinical scenario, an *in vitro* degradation study under hydrolytic conditions was carried out. The results obtained from this test constitute a useful approach to assess the degradation rate of the 3D structures proposed for bone regeneration, as well as a first step in the design of *in vivo* studies.³⁵ Based on the guidelines of ISO standards 10993-9:2019 and 10993-13:2010, a 9-month test was designed using a phosphate buffer saline (PBS) solution as degradation medium. The experiment was conducted in static conditions but replacing the medium monthly to ensure its renewal, mimicking the evacuation of degradation byproducts by fluid flow on *in vivo* conditions.^{35,36} The pH and conductivity of the degradation medium were measured during the test and the scaffolds were characterized in terms of morphological, calorimetric and mechanical properties.

2 | MATERIALS AND METHODS

2.1 | Materials

PLA L105 was purchased in powder form from Corbion Purac (Diemen, The Netherlands). Calcium carbonate (CaCO_3) with a maximum particle size of 30 μm was purchased from VWR (0179-500G). The 3B's Research Group of Universidade do Minho kindly provided β -tricalcium phosphate (β -TCP) particles with a mean size of 45 μm . Aloe vera juice was purchased from Aloe vera Costa Canaria (Costa Canaria Aloe Vera, S.L., Las Palmas, Spain) and hydrochloric (HCl) acid from Panreac (131020, Panreac AppliChem, Darmstadt, Germany).

2.2 | Manufacturing of scaffolds

PLA powder was mixed with the ceramic additives in a ratio of PLA: CaCO_3 : β -TCP 95:2.5:2.5 (wt:wt). This mixture was fed into a lab prototype extruder to obtain continuous filaments with a mean diameter of around 1.75 mm, using the working parameters presented in our previous work.²³ PLA filaments without incorporation of additives were also produced by this method. Then, PLA and composite scaffolds were manufactured by using a BQ Hephestos 2 3D printer (Madrid, Spain), which is based on a material extrusion process (ISO/ASTM 52900:2015), commonly known as fused deposition modeling (FDM). PLA and composite samples without later surface modification are referred in the text as PLA and COMPOSITE groups, respectively.

The scaffolds were manufactured with a 9.8 mm diameter and 7 mm height, with rectangular 0/90° pattern, square-shaped pores and a 50% theoretical porosity. Other printing parameter used include a nozzle diameter of 0.40 mm, a layer height of 0.30 mm, an extrusion width of 0.48 mm, a speed of extrusion of 40 mm/s and a liquefier temperature of 210°C.

2.3 | Application of plasma surface treatment and Aloe vera bioactive coating

Before applying the Aloe vera coating, PLA and composite scaffolds were plasma-treated in a low-pressure device (Zepto Diener electronic GmbH, Ebhausen, Germany) using oxygen as a carrier gas (Carburros Metálicos SA, Madrid, Spain). The oxygen pressure inside the chamber was fixed at 1.8 mbar and the plasma treatment was applied at 30 W for 1 min.

Then, in order to coat the plasma-treated samples, the water-soluble fraction of the centrifuged Aloe vera juice was used. The centrifugation process was carried out at 3000 rpm for 15 min in a Mixtasel-BL centrifuge (JP Selecta S.A., Barcelona, Spain). The separation of the cellulose-rich solid fraction allowed us to obtain a supernatant that contains acetylated polysaccharides, phenolic compounds, soluble carbohydrates, proteins and minerals.^{26,37} Taking into account the results obtained in our previous work,²³ the pH of the obtained solution (measured with a sensIONTM+PH1 pHmeter, ±0.01, HACH) was adjusted to different values to assess the effect of this parameter on the coating process: pH 3 and pH 4 (adjusted with an HCl solution). The acidity of the raw Aloe Vera extract (pH 4.50 ± 0.01) can be explained by the presence of acetic, lactic, succinic, and pyruvic acids.³⁷

The Aloe vera bioactive coating was applied immediately after the plasma treatment. Thus, PLA scaffolds were coated with Aloe vera extracts at pH 3 (PLA AV3), while COMPOSITE scaffolds were coated at pH 3 (COMPOSITE AV3) and 4 (COMPOSITE AV4). To do so, the 3D structures were placed individually in centrifuge tubes (CFT011150, Jet Biofil), immersed in 3 ml of Aloe vera extract solution and stirred at 250 rpm for 3 h. Then, the samples were rinsed with 70% ethanol. The amount of Aloe vera coated on the PLA and composite scaffolds was assessed by measuring the weight of the samples before and after the coating process by using an analytical balance (±0.1 mg, A&D Scales Gemini Series, GR-200, Germany).

2.4 | Hydrolytic degradation study

A static degradation test was carried out under hydrolytic conditions using scaffolds of the five groups proposed: PLA, PLA AV3, COMPOSITE, COMPOSITE AV3, and COMPOSITE AV4. As stated before, all samples were manufactured to have a diameter of 9.8 mm and a height of 7 mm. Twenty-four replicas per group were placed in non-treated 24-well plates (144530, Thermo Scientific™ Nunc™, Waltham, MA, United States) and exposed to UV light for 30 min (15 min per

side of the scaffold) for sterilization purposes. Then, 2 ml of degradation medium were added to each well, comprising a phosphate buffer saline (PBS; 59321C Dulbecco's Phosphate Buffered Saline, pH 7.4, Merck, Darmstadt, Germany) solution with a 0.2 mg/ml concentration of sodium azide (ReagentPlus®, ≥99.5%, Merck, Darmstadt, Germany) to minimize the risk of bacterial contamination.³⁸ Wells without samples but containing degradation medium were used as control.

The well plates were kept in an incubator at 37°C and 5% CO₂ for times up to 1, 3, 6, and 9 months. The buffer solution was replaced monthly, measuring the pH (sensIONTM+PH1, ±0.01, HACH) and conductivity (COND7+, ±0.01, Labbox) of the degradation medium of each group to follow up the evolution of these parameters during the test. At each time point, 6 scaffolds per group were withdrawn for morphological, calorimetric and mechanical characterization. Prior to any of these tests, the samples were dried in a desiccator until complete moisture removal.

2.5 | Morphological characterization

The initial and final weights of the structures were measured using the GR-200 analytical balance to obtain the mean weigh loss after degradation of the scaffolds at each time point. Degraded samples were allowed to dry in a desiccator for at least a week before measuring their final weight. The morphological characterization of these samples included its microscopic observation by scanning electron microscopy (SEM; Hitachi TM 3030, Hitachi Ltd., Tokyo, Japan) at an acceleration voltage of 15 kV. Prior to SEM observation, the samples were sputtered with Pd/Au for 2 min at 18 mA in a SC7620 sputter coater (Polaron, United Kingdom). In addition, the assessment of the pore size (determined as the distance between struts) was carried out by using an Olympus BX51 optical microscope (Olympus Co., Ltd., Tokyo, Japan). Finally, for the evaluation of the porosity of the structures, the following equation was used³⁹:

$$\% \text{porosity} = 100 \cdot \left(1 - \frac{\rho_{\text{ap}}}{\rho_{\text{bulk}}} \right) \quad (1)$$

where ρ_{ap} is the apparent density of the structure and ρ_{bulk} is the density of the bulk material.

2.6 | Calorimetric analysis

Samples extracted from degraded and non-degraded scaffolds were subjected to differential scanning calorimetry (DSC) analysis in DSC 4000 (Perkin Elmer, Waltham, MA, United States). The samples ($n = 4$) were placed in aluminum crucibles and subjected to a heating/cooling/heating cycle from 30 to 230°C. Heating and cooling rates of 10°C/min and a nitrogen flow of 20 ml/min were used. The calorimetric data obtained include the glass transition temperature (T_g), the onset temperature (T_{onset} ; at which the melting process starts), the peak melting temperature (T_{peak}), and the melting enthalpy (ΔH_f).

From the latter value, the crystallinity of each group of samples was estimated according to the following equation:

$$\%X_c = 100 \cdot [\Delta H_f / (\Delta H_f^\circ \cdot W_{PLA})] \quad (2)$$

where X_c is the degree of crystallinity, ΔH_f is the melting enthalpy of the sample, ΔH_f° the melting enthalpy of 100% crystalline PLA and W_{PLA} is the net weight fraction of the PLA in the sample tested. The value used for ΔH_f° was 93.7 J/g.⁴⁰

2.7 | Mechanical characterization

All groups of scaffolds were mechanically characterized in dry state under compression test using a LIYI testing machine (LI-1065, Dongguan Liyi Environmental Technology Co., Ltd., China) in displacement control mode and at a crosshead speed of 1 mm/min. A compression load cell capacity of 500 kg was used. The compressive modulus and offset compressive yield strength were calculated according to ASTM D695-15. In addition, the compression strength, strain at maximum strength and strain at fracture were determined when complete rupture of the specimen occurred during the mechanical test. Non-degraded scaffolds of the PLA and COMPOSITE groups were used as control.

2.8 | Statistical analysis

The statistical analysis was carried out using MATLAB software (MATLAB and Statistics Toolbox Release 2021a, The MathWorks, Inc., Natick, United States). The data obtained during this study were analyzed by the Kruskal-Wallis test, except when only two groups were compared. In the latter case, the Wilcoxon two-sided rank sum test was used. The significance level was set to $*p < .05$, $**p < .01$, and $***p < .001$, for statistically significant, highly statistically

significant, and very highly statistically significant differences, respectively. All figures and tables show the mean values obtained for each group tested. SDs are represented with error bars in the case of figures.

3 | RESULTS AND DISCUSSION

3.1 | Manufacturing of scaffolds and application of surface coatings

All groups of scaffolds were manufactured by FDM using the same printing procedure, as stated in the previous section. The 3D structures obtained were 9.71 ± 10 mm in diameter and 6.82 ± 10 mm in height, having a mean weight of 0.291 ± 0.042 g. After applying the Aloe vera bioactive coating to the PLA and COMPOSITE scaffolds, an average $0.16 \pm 0.02\%$ of weight increase was obtained, as a result of the incorporation of biological substances to the polymeric surface.^{32,33}

3.2 | Conductivity and pH variation during the test

The pH and conductivity variation of the degradation medium during the test for each group of scaffolds are shown in Figures 1 and 2, respectively. The SE of the measurements was around ± 0.01 for both parameters. According to the results, for PLA and composite scaffolds (with or without the Aloe vera coating) the pH of the medium was maintained at a value of around 7.0 during the first 4 months of the experiment. As observed for most of the groups tested, the pH of the degradation medium decreased to a minimum value after 6 months of hydrolytic degradation.

The degradation profile followed by the PLA-based scaffolds evaluated responds to the bulk-erosion autocatalytic mechanism that is characteristic of this biomaterial in hydrolytic

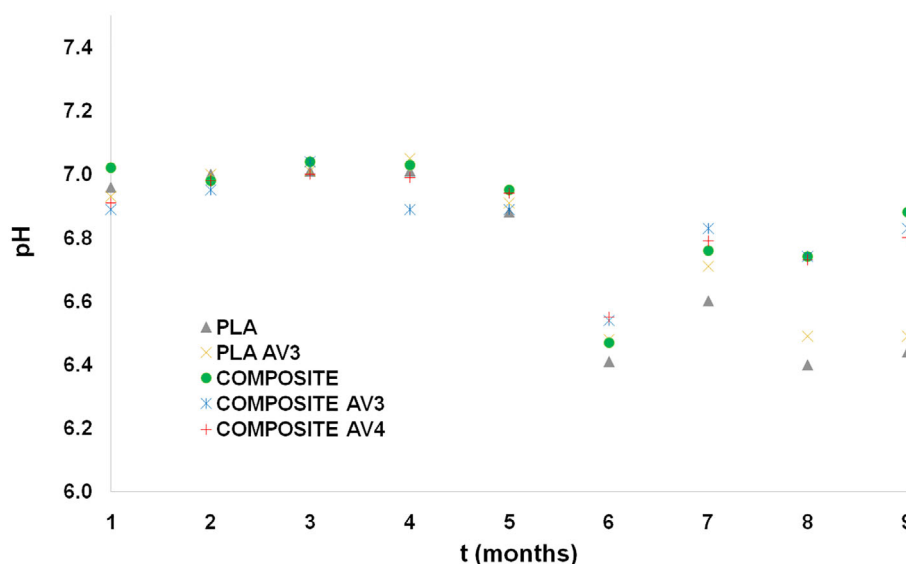
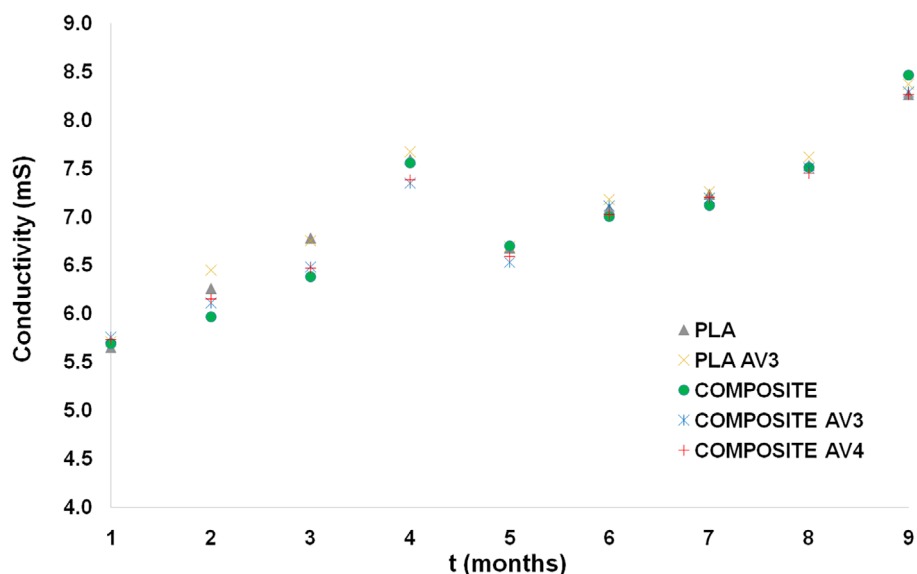


FIGURE 1 Variation of the pH of the medium during the hydrolytic degradation study of the 3D-printed scaffolds

FIGURE 2 Variation of the conductivity (mS) of the medium during the hydrolytic degradation study of the 3D-printed scaffolds



conditions.^{36,38,41,42} In a first step, the absorption of water leads to the hydrolytic cleavage of the polymer chains by breaking the ester bonds. As the first degradation products formed have a relatively high molecular weight, they do not dissolve into the degradation medium and there are a reduced number of chain end groups. Consequently, at this stage, which can be related to the results obtained during the first 4 months of the test, there is no significant change in the weight of the samples. As the hydrolytic process progresses, the molecular weight of the oligomers is reduced to a point at which they can diffuse from the bulk of the material to the surface and then to the aqueous solution. The increased number of chain end groups leads to a significant break of ester bonds, enhancing the degradation rate, the decrease of the pH of the surrounding media and the weight of the structures.^{35,36,42,43} These effects are more significant as the molecular weight decreased, but at the same time the water absorption capacity of the PLA-based structure is also enhanced. The combination of these factors could result in a reduction of the difference on pH values between the inner and outer parts of the scaffolds.⁴³

The second stage described is related to the results obtained from months 4 to 6 (Figure 1). From this point to the end of the experiment the pH of the medium was maintained in the case of PLA samples at a level of around 6.5, whereas composite scaffolds showed an increase in the pH up to 6.88 ± 0.01 for the COMPOSITE group. This result could be explained by the release and dilution of CaCO_3 particles into the PBS solution, which are not only able to compensate acidity, but also acts as a buffer within the physiological pH-range.⁴⁴

The latter conclusions are supported by the conductivity measurements carried out for each group of samples during the test (Figure 2). As for the pH values, non-significant differences were obtained regarding the conductivity of the degradation medium when comparing scaffolds with and without Aloe vera coating. An increased conductivity from month 5 until the end of the test was observed for every group tested. This profile is in accordance with the assumption

TABLE 1 Porosity change of the scaffolds during the hydrolytic degradation test

Group of samples	Time (months)	Porosity (%)
PLA	0	46.6 ± 1.8
	1	47.1 ± 1.8
	3	47.2 ± 2.0
	6	46.5 ± 1.1
	9	51.8 ± 3.0
PLA AV3	0	46.9 ± 1.9
	1	47.5 ± 2.0
	3	47.0 ± 1.9
	6	47.9 ± 1.2
	9	50.8 ± 2.1
COMPOSITE	0	57.4 ± 2.5
	1	57.5 ± 2.8
	3	57.6 ± 2.6
	6	57.5 ± 2.1
	9	57.4 ± 3.0
COMPOSITE AV3	0	57.3 ± 2.2
	1	57.0 ± 2.8
	3	57.9 ± 2.7
	6	57.6 ± 1.7
	9	58.1 ± 2.7
COMPOSITE AV4	0	56.8 ± 2.4
	1	56.9 ± 3.6
	3	57.2 ± 2.9
	6	57.3 ± 2.3
	9	57.8 ± 2.6

Abbreviation: PLA, polylactic acid.

of an increased diffusion and dissolution of low-molecular weight fragments and acidic byproducts (mainly lactic acid); especially relevant between months 5 and 6 (Figure 1).

3.3 | Morphological changes after hydrolytic degradation

In terms of weight loss, non-statistically significant differences were obtained for all groups tested after 9 months of hydrolytic degradation. The mean weight loss of the scaffolds at the end of the experiment was equal to $0.30 \pm 0.11\%$. On the other hand, results regarding the porosity of the 3D structures (calculated according to Equation (1), presented in Section 2.5) are summarized in Table 1. From the measurement of the mass and dimensions of short filaments of material ($n = 8$), values of ρ_{bulk} were estimated to be $1.22 \pm 0.03 \text{ g/cm}^3$, and $1.25 \pm 0.02 \text{ g/cm}^3$ for PLA and COMPOSITE samples, respectively. The apparent density was calculated following a similar procedure for the 3D-printed scaffolds.

As shown in our previous studies,^{13,45} the surface roughness and microporosity of 3D-printed COMPOSITE filaments are significantly higher compared to PLA scaffolds, leading to an enhanced overall porosity of the manufactured structures (Table 1). A similar statement was presented by Esposito Corcione et al.,⁴⁶ who concluded that the introduction of a ceramic phase (HAp) into a PLA matrix led to a higher porosity of their PLA/HAp 3D-printed scaffolds (compared to the pure PLA-ones) caused by a superior surface roughness and intrinsic porosity of the composite struts.

According to Table 1 and despite being not statistically significant, the PLA and PLA AV3 groups showed a porosity increase from months 6 to 9. These results seem to contradict the ones presented in Figure 3, related to the pore size of the scaffolds during the degradation test. However, the significant pore size reduction observed for the PLA and PLA AV3 groups are attributed to the statistically

significant increase of the scaffold's dimensions obtained for these structures: as the degradation of the base material progresses, more hydrophilic chain ends are generated, enhancing the water uptake and causing the biomaterial to swell.⁴³ Overall, the increase in the microporosity of the PLA struts during degradation had a more important effect than the reduction in pore size due to swelling, leading to an increase in the porosity of the scaffolds at the end of the test. From Figure 3, it is also worth noticing that the composite scaffolds possess an initially higher pore size than the PLA scaffold groups (not statistically significant difference), which implies a smaller diameter of the composite printed struts. This is another reason for the superior porosity of the composite scaffold groups (Table 1).⁴⁵

SEM observations (Figure 4) confirmed the modifications generated by the degradation process on the polymeric surface of the PLA samples. Numerous fractures were observed for PLA scaffolds after 9 months of degradation (Figure 4C), which some authors have related to the orientation gradient of the polymeric chains imposed by the manufacturing technique; as the degradation rate of polyhydroxy acids decreased with increasing chain orientation (the less-oriented center of the piece degrades before the outer oriented region).³⁶ In addition, the limited diffusion of the acidic byproducts throughout the 3D structure contributes to inhomogeneous degradation of the part.⁵

In the case of composite groups of scaffolds, no fractures were observed on the degraded surface (Figure 4F). During degradation, the presence of ceramic particles seems to prevent the propagation of cracks in the polymeric matrix, as stated by Senatov et al.^{46,47} Furthermore, and in contrast to PLA scaffolds, composite groups showed non-statistically significant variation through the degradation test in terms of porosity, pore size nor dimensions, thus maintaining the

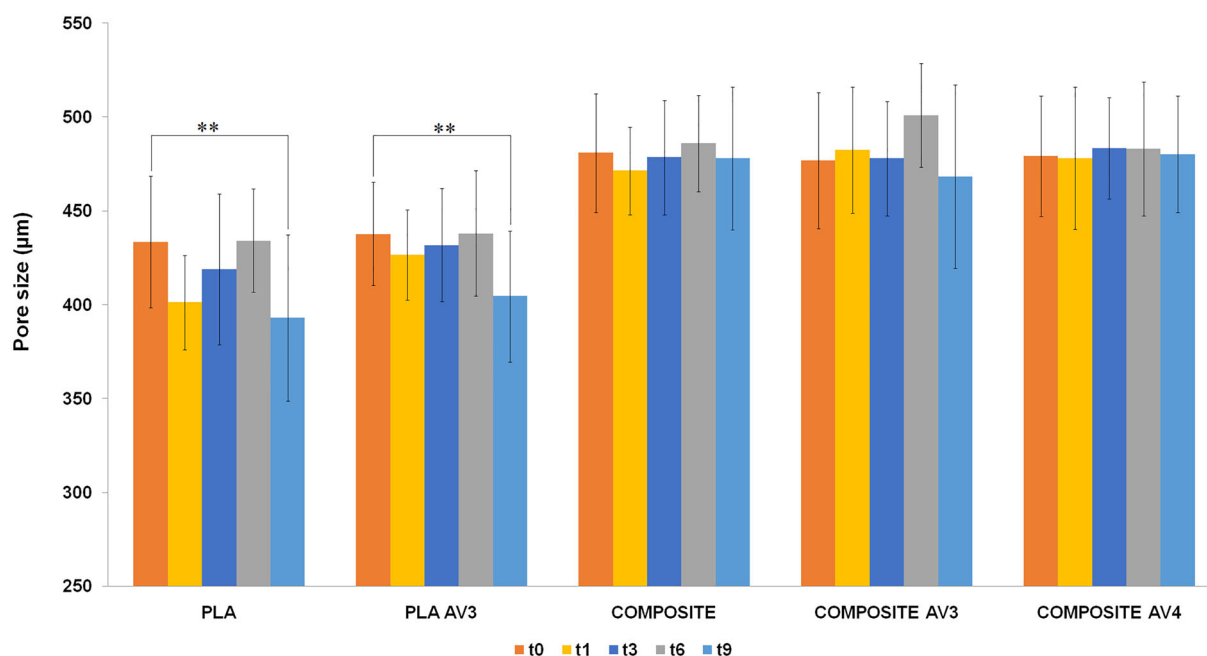


FIGURE 3 Pore size values of the 3D-printed scaffolds degraded under hydrolytic conditions (** $p < .01$)

initial properties for a time up to 9 months. The latter is true for both non-treated (COMPOSITE group) and surface-treated composite scaffolds (COMPOSITE AV3 and COMPOSITE AV4 groups), suggesting that the Aloe vera coating method applied had no effect on the morphology of the 3D-printed structures. In the same way, non-significant differences were observed when comparing the morphological characteristics of the PLA and PLA AV3 groups of samples.

3.4 | Calorimetric properties and crystallinity assessment

All groups of scaffolds tested showed a continuous reduction of their calorimetric properties during the degradation test (Table 2). The decrease in the glass, onset and peak melting temperatures was more pronounced for PLA and PLA AV3 samples than for the COMPOSITE, COMPOSITE AV3 and COMPOSITE AV4 groups. For example, the melting temperature of PLA scaffolds was reduced from $175.9 \pm 0.3^\circ\text{C}$ to $163.1 \pm 1.7^\circ\text{C}$ after 9 months, while COMPOSITE scaffolds showed a mean melting temperature of $168.5 \pm 3.9^\circ\text{C}$ at the end of the experiment. In addition, non-significant differences were obtained between the non-treated and coated samples. Therefore, the Aloe

vera bioactive coating applied to the 3D structures showed no effect on the calorimetric properties of the base material.

The degree of crystallinity, calculated from the mean value of melting enthalpy of each group, is enhanced by the introduction of the ceramic additives into the PLA matrix due to nucleation effect.^{40,48,49} According to the results presented in Table 2, this parameter was increased from a value of $51.5 \pm 2.6\%$ for non-degraded PLA scaffolds to $54.5 \pm 1.9\%$ for the COMPOSITE group at $t = 0$.

Regarding the variation of the degree of crystallinity, this value was continuously increasing during the 9-month test for PLA and PLA AV3 groups, while no clear tendency was observed for composite scaffolds. The increase of the crystallinity was an expected result, as have been shown for semi-crystalline polymers, such as PLA, during the early stages of a hydrolytic degradation process.^{36,38,50} The latter effect could be attributed to^{35,36,51}: (a) the plasticization effect, since the absorption of water molecules favors the movement of the polymeric chains located in the amorphous region, leading to their rearrangement to a crystalline structure; (b) during the early stages, degradation occurs preferentially in the amorphous regions, which are more accessible to water molecules; and (c) the generation of crystalline monomers and oligomers during the degradation process. In the

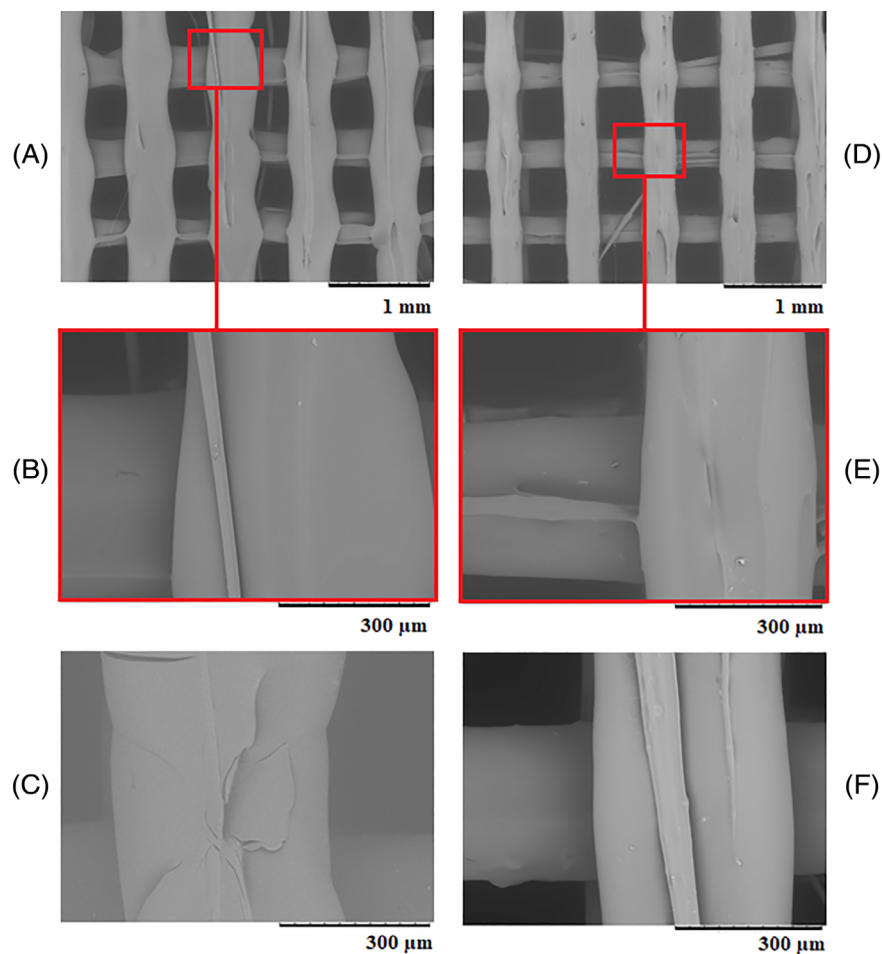


FIGURE 4 Scanning electron microscopy (SEM) images of the 3D-printed poly(lactic acid) (PLA)-based scaffolds analyzed are shown for: (A) non-degraded PLA; (B) non-degraded PLA at higher magnification; (C) PLA at $t = 9$ months; (D) non-degraded COMPOSITE; (E) non-degraded COMPOSITE at higher magnification; and (F) COMPOSITE at $t = 6$ months

last stages, chain cleavage in the crystalline region occurs, producing a decrease in the crystallinity of the base material.^{35,36}

3.5 | Mechanical properties under compression

Results regarding the compression test of the degraded scaffolds are shown in Table 3. The addition of the ceramic additives led to a significant reduction of the elastic modulus: from 122.23 ± 6.44 MPa to 77.72 ± 16.09 MPa for PLA and COMPOSITE groups, respectively. The same conclusion is drawn from the compressive yield strength results, as this parameter decreased nearly by half for COMPOSITE scaffolds (7.41 ± 1.77 MPa) in comparison to neat PLA scaffolds (14.28 ± 2.65 MPa). While references in the literature can be found where use of ceramic additives strengthens the polymeric matrix,^{46,52} other authors have also encountered a reduction in the mechanical properties of composite PLA scaffolds⁴⁵ in comparison to their pure PLA control. Such result can be explained taking into account the morphological findings presented in Section 3.3: composite scaffolds showed higher overall porosity due to their smaller, more porous and rougher

printed struts. The decrease in mechanical properties with increasing scaffold porosity is in good correlation with the literature.^{53,54} Despite not being able to reinforce the polymeric matrix, the ceramic additives used are increasing the available surface area of the PLA structure,⁴⁵ which is a feature of great interest for their application in the BTE field. In addition, both elastic modulus and compressive yield strength of COMPOSITE scaffolds are still in the range of values reported for cancellous bone.^{3,55}

On the other hand, the Aloe vera bioactive coatings applied to the structures showed no effect on the mechanical properties. Hence, the procedure proposed to modify the polymeric surface allows to improve the biological properties of the sample, as we have demonstrated in our previous study,²³ without diminishing the mechanical support provided by the 3D structure.

Degraded PLA and PLA AV3 scaffolds showed a slight reduction in terms of elastic modulus and compressive yield strength during the first 6 months of hydrolytic degradation. Then, a highly statistically significant decrease ($p < .01$) was obtained for both parameters. Since the first steps of bulk degradation of PLA takes place in the amorphous regions,^{36,38,50} a reduction in molecular weight is expected

TABLE 2 Calorimetric properties determined by DSC analysis of the degraded PLA-based scaffolds

Group of samples	Time (months)	T_g (°C)	T_{onset} (°C)	T_{peak} (°C)	ΔH_f (J/g)	% X_c
PLA	0	63.6 ± 0.9	167.8 ± 2.7	175.9 ± 0.3	48.3 ± 2.5	51.5 ± 2.6
	1	64.5 ± 0.6	164.1 ± 2.0	175.4 ± 1.4	49.9 ± 3.8	53.2 ± 4.1
	3	64.3 ± 0.6	163.2 ± 2.0	174.0 ± 1.4	48.7 ± 3.8	52.0 ± 4.1
	6	61.3 ± 0.6	161.4 ± 0.4	172.2 ± 2.2	50.4 ± 3.9	53.8 ± 4.2
	9	52.0 ± 0.3	154.2 ± 2.7	163.1 ± 1.7	51.4 ± 5.1	54.9 ± 5.4
PLA AV3	0	63.7 ± 0.0	167.0 ± 3.1	176.2 ± 0.7	44.7 ± 7.0	47.7 ± 7.5
	1	63.4 ± 0.6	169.1 ± 3.3	175.2 ± 1.9	50.2 ± 3.8	53.5 ± 4.0
	3	63.7 ± 0.6	163.2 ± 3.3	173.8 ± 1.9	50.8 ± 3.8	54.2 ± 4.0
	6	59.8 ± 0.9	161.1 ± 0.6	172.1 ± 2.0	51.2 ± 1.8	54.6 ± 1.9
	9	52.5 ± 0.9	159.3 ± 6.3	165.4 ± 3.1	52.4 ± 2.5	55.9 ± 2.7
COMPOSITE	0	63.6 ± 0.3	167.7 ± 3.4	175.8 ± 0.6	48.5 ± 1.7	54.5 ± 1.9
	1	63.7 ± 1.4	168.5 ± 1.4	175.1 ± 1.6	46.1 ± 2.6	51.8 ± 2.9
	3	63.0 ± 1.4	169.0 ± 1.4	174.9 ± 1.6	45.7 ± 2.6	51.3 ± 2.3
	6	60.7 ± 0.1	162.7 ± 0.2	173.0 ± 0.2	45.9 ± 2.0	51.5 ± 4.5
	9	58.2 ± 3.9	162.2 ± 0.5	168.5 ± 3.9	49.1 ± 4.0	55.2 ± 3.0
COMPOSITE AV3	0	63.8 ± 1.9	169.9 ± 0.5	176.1 ± 0.6	46.6 ± 2.7	52.3 ± 3.0
	1	61.9 ± 1.9	169.0 ± 0.5	175.3 ± 0.6	44.1 ± 2.7	49.5 ± 3.0
	3	60.6 ± 1.9	168.7 ± 0.5	174.7 ± 0.6	51.1 ± 2.7	57.4 ± 3.0
	6	60.8 ± 0.6	162.8 ± 0.3	173.6 ± 0.6	44.0 ± 2.9	49.5 ± 3.2
	9	61.2 ± 3.2	161.7 ± 0.6	166.1 ± 0.5	50.0 ± 2.4	56.2 ± 2.7
COMPOSITE AV4	0	61.3 ± 0.4	170.0 ± 0.4	176.0 ± 0.6	44.0 ± 3.1	49.4 ± 3.5
	1	63.6 ± 0.4	168.9 ± 0.4	176.1 ± 0.6	46.2 ± 3.1	51.9 ± 3.5
	3	60.8 ± 0.4	167.0 ± 0.4	173.9 ± 0.6	49.9 ± 3.1	56.0 ± 3.5
	6	61.3 ± 0.4	162.7 ± 0.3	173.1 ± 0.5	48.9 ± 1.3	55.0 ± 1.5
	9	60.5 ± 0.5	161.9 ± 0.5	166.0 ± 0.6	46.1 ± 4.9	51.8 ± 5.5

Abbreviations: DSC, differential scanning calorimetry; PLA, polylactic acid.

TABLE 3 Calorimetric properties determined by DSC analysis of the degraded PLA-based scaffolds

Group of samples	Time (months)	Elastic modulus (MPa)	Compressive yield strength (MPa)	Compression strength (MPa)	Strain at maximum strength	Strain at fracture
PLA	0	122.23 ± 6.44	14.28 ± 2.65	-	-	-
	1	127.44 ± 5.18	15.75 ± 2.21	-	-	-
	3	121.09 ± 0.52	14.37 ± 1.23	15.03 ± 0.90	0.188 ± 0.017	0.197 ± 0.025
	6	114.30 ± 4.47	11.65 ± 1.16	12.40 ± 1.58	0.159 ± 0.013	0.164 ± 0.014
	9	32.12 ± 12.06 ^a	2.35 ± 0.95 ^a	2.42 ± 0.97 ^b	0.104 ± 0.013 ^b	0.110 ± 0.012 ^b
PLA AV3	0	122.23 ± 6.44	14.28 ± 2.65	-	-	-
	1	125.81 ± 3.78	14.77 ± 0.63	-	-	-
	3	116.32 ± 11.65	13.52 ± 4.34	13.96 ± 4.46	0.190 ± 0.054	0.201 ± 0.058
	6	103.14 ± 15.22	10.39 ± 2.75	11.18 ± 2.42	0.172 ± 0.012	0.178 ± 0.011
	9	36.46 ± 7.68 ^c	2.45 ± 0.83 ^d	2.73 ± 0.64 ^e	0.110 ± 0.008 ^e	0.115 ± 0.008 ^e
COMPOSITE	0	77.72 ± 16.09	7.41 ± 1.77	-	-	-
	1	82.36 ± 7.13	7.89 ± 1.36	-	-	-
	3	85.76 ± 9.46	7.91 ± 0.98	-	-	-
	6	82.63 ± 2.97	7.90 ± 0.34	10.57 ± 1.63	0.278 ± 0.109	0.303 ± 0.119
	9	85.23 ± 8.24	7.85 ± 1.61	8.47 ± 1.69	0.161 ± 0.019 ^f	0.165 ± 0.020 ^f
COMPOSITE AV3	0	77.72 ± 16.09	7.41 ± 1.77	-	-	-
	1	88.75 ± 12.78	8.12 ± 1.50	-	-	-
	3	76.87 ± 3.24	7.13 ± 0.21	-	-	-
	6	85.26 ± 4.43	7.89 ± 0.83	9.36 ± 0.82	0.184 ± 0.034	0.203 ± 0.049
	9	82.33 ± 5.59	8.08 ± 1.46	8.59 ± 1.53	0.159 ± 0.027	0.166 ± 0.032
COMPOSITE AV4	0	77.72 ± 16.09	7.41 ± 1.77	-	-	-
	1	87.31 ± 13.70	8.62 ± 1.87	-	-	-
	3	81.12 ± 5.11	6.99 ± 0.19	-	-	-
	6	82.98 ± 6.24	8.25 ± 1.46	10.10 ± 2.40	0.231 ± 0.074	0.250 ± 0.089
	9	84.35 ± 6.37	7.84 ± 1.43	8.27 ± 1.43	0.151 ± 0.023	0.155 ± 0.024

Abbreviations: DSC, differential scanning calorimetry; PLA, polylactic acid.

^a***p* < .01 compared with samples at *t* = 1 month.

^b***p* < .01 compared with samples at *t* = 3 months.

^c**p* < .05 compared with samples at *t* = 0 months and ***p* < .01 compared samples at *t* = 1 month.

^d**p* < .05 compared with samples at *t* = 1 month.

^e**p* < .05 compared with samples at *t* = 3 months.

^f**p* < .05 compared with samples at *t* = 6 months.

without a loss of mechanical properties; which are more related to the crystalline phase.² In contrast, the advanced stages of degradation are characterized by a marked decrease in molecular weight, weight of the structure and crystallinity of the base material, and consequently in the mechanical properties of the 3D-structure.^{2,35} PLA and PLA AV3 scaffolds tested showed no such reductions in terms of weight or crystallinity (Table 2) after 9 months of degradation. Thus, the decrease in mechanical properties observed could be related to the degradation of amorphous regions located between crystalline zones^{56,57}: the increasing density of terminal groups during the degradation of PLA leads to a reduction of polymeric chain's packing and the increase of the water absorption (Figure 3), enhancing the hydrolytic process in the amorphous regions located between crystalline zones; which produces the loss of the mechanical properties even before the crystalline regions start to degrade.

Conversely, COMPOSITE scaffolds and Aloe vera coated composite groups maintained their mechanical properties until the end of the test. An example of the difference observed between PLA and COMPOSITE groups is presented in Figure 5. Noteworthy, the break point of the PLA and PLA AV3 scaffolds was reached at the 3-month compression test (displacement equal to 2 mm as stop condition), while composite scaffolds did not collapse until the mechanical test carried out in month 6 (Table 3). Even after 9 months of hydrolytic degradation, the compression strength of non-treated and Aloe vera coated composite scaffolds had a value around 8 MPa, therefore in the range of cancellous bone.^{3,55} We hypothesize that the nucleation effect provided by the ceramic additives^{41,48,49} could have produced a partial crystallization (Table 2) in amorphous areas located between crystalline regions, thus favoring the maintenance of the mechanical support until the degradation process reaches its final stages.

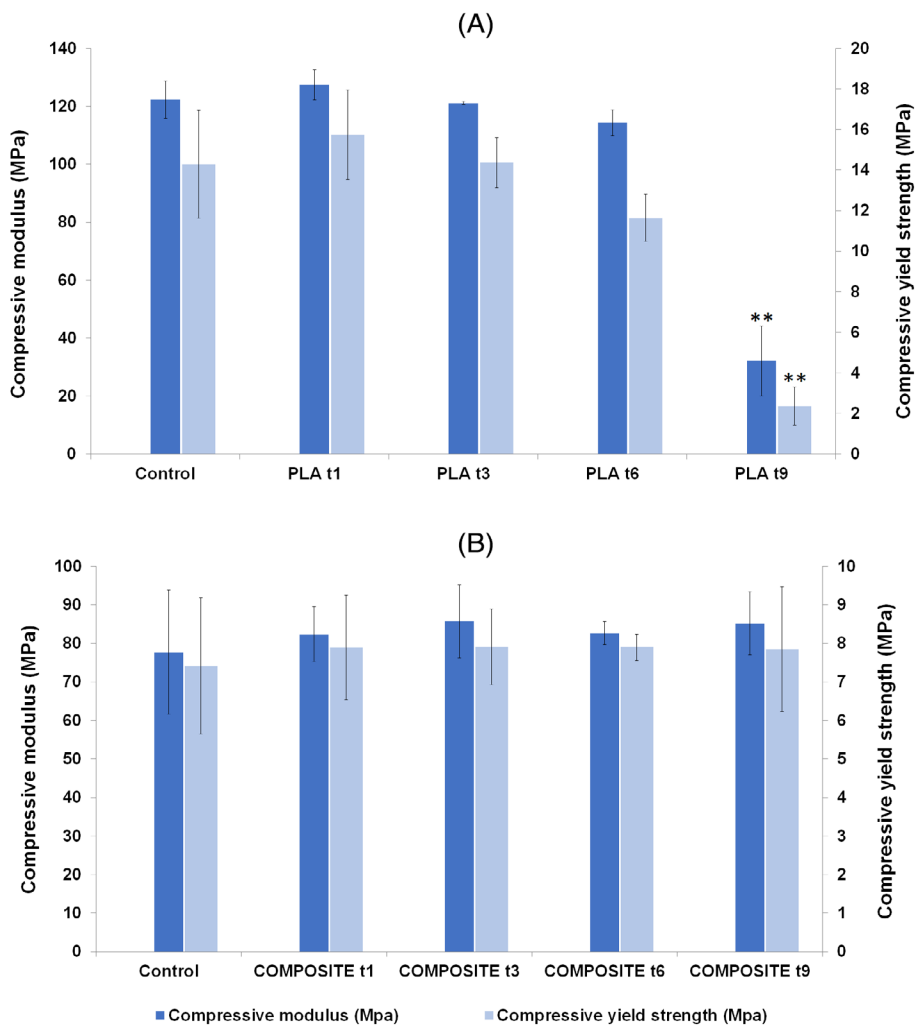


FIGURE 5 Mechanical properties under compression testing of the degraded 3D-printed scaffolds: (A) polylactic acid (PLA) and (B) COMPOSITE (** $p < .01$ compared with the PLA t1 group of samples)

4 | CONCLUSIONS

According to the results obtained after the degradation test, composite scaffolds showed non-significant differences in terms of pore size, porosity or mechanical properties. While initially lower than for PLA scaffolds, the mechanical characteristics of the composite 3D structures evaluated can match the ones required for cancellous bone regeneration,⁵⁵ even after 9 months of hydrolytic degradation. In addition, the release of ceramic particles allowed maintaining a slightly higher pH of the degradation medium in comparison to neat PLA scaffolds. As in vivo degradation of PLA samples takes place following a hydrolytic degradation mechanism,^{2,36} the test carried out provides essential information for understanding the behavior of the scaffolds in a close-to-clinic situation. The maintenance of the pH level of the surrounding medium is of utmost importance in the case of PLA-based implants, as the abrupt release of acidic byproducts or its inefficient removal could generate a strong inflammatory response, thus hindering cell viability, growth and proliferation.^{7,42}

On the other hand, the Aloe vera coating methods evaluated had no effect on the bulk properties of the 3D-structure. The latter, however, have shown to improve the biofunctionality of PLA-based scaffolds, as presented in one of our previous studies,²³ leading to an

enhanced cell proliferation of osteoblastic cells cultured in vitro. Thus, while it is not expected to have a major effect in the long term, the bioactive coating applied seems to favor early steps of bone regeneration, when cell-material interactions are primarily dictated by surface properties.⁵⁸ Further research is needed to understand for how long the coating remains and which is the mechanism of detachment. Nevertheless, with the results obtained so far, it could be concluded that the synergetic effect of both Aloe vera bioactive coating and ceramic additives would allow obtaining a 3D structure with improved biological efficacy right after implantation (thanks to the coating) as well as adequate maintenance of mechanical support and controlled degradation after a long period (due to the presence of the additives). Hence, this work shows the potential of composite PLA-based scaffolds, manufactured by AM and surface-modified to attach bioactive compounds, to be further evaluated for BTE applications.

CRedit STATEMENT

Ricardo Donate: Conceptualization, methodology, formal analysis, investigation, writing—original draft, visualization. **Mario Monzón:** Resources, writing—review and editing, supervision, project administration, funding acquisition. **María Elena Alemán-Domínguez:** Methodology, investigation, writing—review and editing. **Francisco**

Rodríguez-Esparragón: Resources, writing—review and editing. All authors have read and approved this manuscript for publication.

ACKNOWLEDGMENTS

This contribution is part of the BioAM project (DPI2017-88465-R) funded by the Science, Innovation and Universities Spanish Ministry. Also, the authors would like to acknowledge the support of the Spanish Ministry of Science and Innovation for funding the UNLP10-3E-726 infrastructure project, co-financed with ERDF funds. Ricardo Donate express his gratitude for the funding through the PhD grant program co-financed by the Canarian Agency for Research, Innovation and Information Society of the Canary Islands Regional Council for Employment, Industry, Commerce and Knowledge and by the European Social Fund (ESF) Canary Islands Integrated Operational Program 2014-2020, Axis 3 Priority Theme 74 (85%). Grant code: TESIS2017010036.

CONFLICT OF INTEREST

The authors declare no conflict of interest. The funders had no role in the design of the study; in the collection, analyses, or interpretation of data; in the writing of the manuscript, or in the decision to publish the results.

DATA AVAILABILITY STATEMENT

The data presented in this study are available on request from the corresponding author.

ORCID

Ricardo Donate  <https://orcid.org/0000-0002-4337-5991>

REFERENCES

- Tajbakhsh S, Hajiali F. A comprehensive study on the fabrication and properties of biocomposites of poly(lactic acid)/ceramics for bone tissue engineering. *Mater Sci Eng C*. 2017;70:897-912. doi:10.1016/j.msec.2016.09.008
- Farah S, Anderson DG, Langer R. Physical and mechanical properties of PLA, and their functions in widespread applications—a comprehensive review. *Adv Drug Deliv Rev*. 2016;107:367-392. doi:10.1016/j.addr.2016.06.012
- Narayanan G, Vernekar VN, Kuyinu EL, Laurencin CT. Poly (lactic acid)-based biomaterials for orthopaedic regenerative engineering. *Adv Drug Deliv Rev*. 2016;107:247-276. doi:10.1016/j.addr.2016.04.015
- Zhou H, Touny AH, Bhaduri SB. Fabrication of novel PLA/CDHA bio-nanocomposite fibers for tissue engineering applications via electrospinning. *J Mater Sci Mater Med*. 2011;22:1183-1193. doi:10.1007/s10856-011-4295-6
- Ginjurpalli K, Shavi GV, Averineni RK, Bhat M, Udupa N, Nagaraja UP. Poly(α -hydroxy acid) based polymers: a review on material and degradation aspects. *Polym Degrad Stab*. 2017;144:520-535. doi:10.1016/j.polymdegradstab.2017.08.024
- Janorkar AV, Metters AT, Hirt DE. Modification of poly(lactic acid) films: enhanced wettability from surface-confined photografting and increased degradation rate due to an artifact of the photografting process. *Macromolecules*. 2004;37:9151-9159. doi:10.1021/ma049056u
- Araque-Monrós MC, Vidaurre A, Gil-Santos L, Gironés Bernabé S, Monleón-Pradas M, Más-Estellés J. Study of the degradation of a new PLA braided biomaterial in buffer phosphate saline, basic and acid media, intended for the regeneration of tendons and ligaments. *Polym Degrad Stab*. 2013;98:1563-1570. doi:10.1016/j.polymdegradstab.2013.06.031
- McMillan R, Meeks B, Bensebaa F, Deslandes Y, Sheardown H. Engineering new bone tissue in vitro on highly porous poly(α -hydroxyl acids)/hydroxyapatite composite scaffolds. *J Biomed Mater Res*. 2001;54:284-293. doi:10.1002/1097-4636(200102)54:23.0.CO;2-W
- Lin PL, Fang HW, Tseng T, Lee WH. Effects of hydroxyapatite dosage on mechanical and biological behaviors of polylactic acid composite materials. *Mater Lett*. 2007;61:3009-3013. doi:10.1016/j.matlet.2006.10.064
- Jeong SI, Ko EK, Yum J, Jung CH, Lee YM, Shin H. Nanofibrous poly(lactic acid)/hydroxyapatite composite scaffolds for guided tissue regeneration. *Macromol Biosci*. 2008;8:328-338. doi:10.1002/mabi.200700107
- Lou T, Wang X, Song G, Gu Z, Yang Z. Structure and properties of PLLA/ β -TCP nanocomposite scaffolds for bone tissue engineering. *J Mater Sci Mater Med*. 2015;26:1-7. doi:10.1007/s10856-014-5366-2
- McCullen SD, Zhu Y, Bernacki SH, et al. Electrospun composite poly(L-lactic acid)/tricalcium phosphate scaffolds induce proliferation and osteogenic differentiation of human adipose-derived stem cells. *Biomed Mater*. 2009;4:035002. doi:10.1088/1748-6041/4/3/035002
- Donate R, Monzón M, Ortega Z, et al. Comparison between calcium carbonate and β -tricalcium phosphate as additives of 3D printed scaffolds with polylactic acid matrix. *J Tissue Eng Regen Med*. 2020;14:272-283. doi:10.1002/term.2990
- Wang M, Favi P, Cheng X, et al. Cold atmospheric plasma (CAP) surface nanomodified 3D printed polylactic acid (PLA) scaffolds for bone regeneration. *Acta Biomater*. 2016;46:256-265. doi:10.1016/j.actbio.2016.09.030
- Woo KM, Seo J, Zhang R, Ma PX. Suppression of apoptosis by enhanced protein adsorption on polymer/hydroxyapatite composite scaffolds. *Biomaterials*. 2007;28:2622-2630. doi:10.1016/j.biomaterials.2007.02.004
- Chen WY, Matthews A, Jones FR, Chen KS. Immobilization of carboxylic acid groups on polymeric substrates by plasma-enhanced chemical vapor or atmospheric pressure plasma deposition of acetic acid. *Thin Solid Films*. 2018;666:54-60. doi:10.1016/j.tsf.2018.07.051
- Zhang X, Lou Q, Wang L, Min S, Zhao M, Quan C. Immobilization of BMP-2-derived peptides on 3D-printed porous scaffolds for enhanced osteogenesis. *Biomed Mater*. 2019;15(1):015002. doi:10.1088/1748-605X/ab4c78
- Yanoso-Scholl L, Jacobson JA, Bradica G, et al. Evaluation of dense polylactic acid/beta-tricalcium phosphate scaffolds for bone tissue engineering. *J Biomed Mater Res - Part A*. 2010;95:717-726. doi:10.1002/jbm.a.32868
- Yang Z, Si J, Cui Z, et al. Biomimetic composite scaffolds based on surface modification of polydopamine on electrospun poly(lactic acid)/cellulose nanofibrils. *Carbohydr Polym*. 2017;174:750-759. doi:10.1016/j.carbpol.2017.07.010
- Xu Y, Huang Z, Pu X, Yin G, Zhang J. Fabrication of chitosan/polypyrrole-coated poly(L-lactic acid)/polycaprolactone aligned fibre films for enhancement of neural cell compatibility and neurite growth. *Cell Prolif*. 2019;52:1-12. doi:10.1111/cpr.12588
- Sultana N, Wang M. PHBV/PLLA-based composite scaffolds fabricated using an emulsion freezing/freeze-drying technique for bone tissue engineering: surface modification and in vitro biological evaluation. *Biofabrication*. 2012;4:015003. doi:10.1088/1758-5082/4/1/015003
- Luo Y, Humayun A, Mills DK. Surface modification of 3D printed PLA/halloysite composite scaffolds with antibacterial and osteogenic capabilities. *Appl Sci*. 2020;10:3971. doi:10.3390/app10113971

23. Donate R, Alemán-Domínguez ME, Monzón M, Yu J, Rodríguez-Esparragón F, Liu C. Evaluation of aloe vera coated polylactic acid scaffolds for bone tissue engineering. *Appl Sci*. 2020;10:2576. doi:10.3390/APP10072576
24. Choi S, Chung MH. A review on the relationship between aloe vera components and their biologic effects. *Semin Integr Med*. 2003;1:53-62. doi:10.1016/S1543-1150(03)00005-X
25. Gao Y, Kuok KI, Jin Y, Wang R. Biomedical applications of Aloe vera. *Crit Rev Food Sci Nutr*. 2019;59:S244-S256. doi:10.1080/10408398.2018.1496320
26. Femenia A, Sánchez ES, Simal S, Rosselló C. Compositional features of polysaccharides from Aloe vera (*Aloe barbadensis* Miller) plant tissues. *Carbohydr Polym*. 1999;39:109-117. doi:10.1016/S0144-8617(98)00163-5
27. Godoy DJD, Chokboribal J, Pauwels R, et al. Acemannan increased bone surface, bone volume, and bone density in a calvarial defect model in skeletally-mature rats. *J Dent Sci*. 2018;13:334-341. doi:10.1016/j.jds.2018.06.004
28. Boonyagul S, Banlunara W, Sangvanich P, Thunyakitpisal P. Effect of acemannan, an extracted polysaccharide from Aloe vera, on BMSCs proliferation, differentiation, extracellular matrix synthesis, mineralization, and bone formation in a tooth extraction model. *Odontology*. 2014;102:310-317. doi:10.1007/s10266-012-0101-2
29. Baghersad S, Hajir Bahrami S, Mohammadi MR, Mojtahedi MRM, Milan PB. Development of biodegradable electrospun gelatin/aloe-vera/poly(ϵ -caprolactone) hybrid nanofibrous scaffold for application as skin substitutes. *Mater Sci Eng C*. 2018;93:367-379. doi:10.1016/j.msec.2018.08.020
30. Jouybar A, Seyedjafari E, Ardashirylajimi A, et al. Enhanced skin regeneration by herbal extract-coated poly-L-lactic acid NANOFIBROUS scaffold. *Artif Organs*. 2017;41:E296-E307. doi:10.1111/aor.12926
31. Ezhilarasu H, Ramalingam R, Dhand C, et al. Biocompatible aloe vera and tetracycline hydrochloride loaded hybrid nanofibrous scaffolds for skin tissue engineering. *Int J Mol Sci*. 2019;20:5174. doi:10.3390/ijms20205174
32. Wang H, Zhang X, Mani MP, Jaganathan SK, Huang Y, Wang C. Microwave-assisted dip coating of Aloe vera on metallocene polyethylene incorporated with nano-rods of hydroxyapatite for bone tissue engineering. *Coatings*. 2017;7:182. doi:10.3390/coatings7110182
33. Banerjee D, Bose S. Effects of aloe vera gel extract in doped hydroxyapatite-coated titanium implants on in vivo and in vitro biological properties. *ACS Appl Bio Mater*. 2019;2:3194-3202. doi:10.1021/acsabm.9b00077
34. Tahmasebi A, Shapouri Moghadam A, Enderami SE, et al. Aloe vera-derived gel-blended PHBV nanofibrous scaffold for bone tissue engineering. *ASAIO J*. 2020;66:966-973. doi:10.1097/MAT.0000000000001094
35. Azevedo H, Reis R. Understanding the enzymatic degradation of biodegradable polymers and strategies to control their degradation rate. *Biodegrad Syst Tissue Eng Regen Med*. 2004;177-202. doi:10.1201/9780203491232.ch12
36. Mainil-Varlet P, Curtis R, Gogolewski S. Effect of in vivo and in vitro degradation on molecular and mechanical properties of various low-molecular-weight polylactides. *J Biomed Mater Res*. 1997;36:360-380. doi:10.1002/(SICI)1097-4636(19970905)36:33.0.CO;2-I
37. Monakhova YB, Randel G, Diehl BWK. Automated control of the organic and inorganic composition of Aloe vera extracts using ¹H NMR spectroscopy. *J AOAC Int*. 2016;99:1213-1218. doi:10.5740/jaoacint.16-0020
38. Tsuji H, Muramatsu H. Blends of aliphatic polyesters: V. Non-enzymatic and enzymatic hydrolysis of blends from hydrophobic poly(L-lactide) and hydrophilic poly(vinyl alcohol). *Polym Degrad Stab*. 2001;71:403-413. doi:10.1016/S0141-3910(00)00192-0
39. Domingos M, Intranuovo F, Gloria A, et al. Improved osteoblast cell affinity on plasma-modified 3-D extruded PCL scaffolds. *Acta Biomater*. 2013;9:5997-6005. doi:10.1016/j.actbio.2012.12.031
40. Garlotta D. A literature review of poly(lactic acid). *J Polym Environ*. 2001;9:63-84. doi:10.1023/A:1020200822435
41. Li S, McCarthy S. Influence of crystallinity and stereochemistry on the enzymatic degradation of poly(lactide)s. *Macromolecules*. 1999;32:4454-4456. doi:10.1021/ma990117b
42. Yildirimer L, Seifalian AM. Three-dimensional biomaterial degradation—material choice, design and extrinsic factor considerations. *Biotechnol Adv*. 2014;32:984-999. doi:10.1016/j.biotechadv.2014.04.014
43. Lyu SP, Untereker D. Degradability of polymers for implantable biomedical devices. *Int J Mol Sci*. 2009;10:4033-4065. doi:10.3390/ijms10094033
44. Schiller C, Epple M. Carbonated calcium phosphates are suitable pH-stabilising fillers for biodegradable polyesters. *Biomaterials*. 2003;24:2037-2043. doi:10.1016/S0142-9612(02)00634-8
45. Esposito Corcione C, Gervaso F, Scalera F, et al. Highly loaded hydroxyapatite microsphere/PLA porous scaffolds obtained by fused deposition modelling. *Ceram Int*. 2019;45:2803-2810. doi:10.1016/j.ceramint.2018.07.297
46. Senatov FS, Niaza KV, Zadorozhnyy MY, Maksimkin AV, Kaloshkin SD, Estrin YZ. Mechanical properties and shape memory effect of 3D-printed PLA-based porous scaffolds. *J Mech Behav Biomed Mater*. 2016;57:139-148. doi:10.1016/j.jmbbm.2015.11.036
47. Senatov FS, Niaza KV, Stepashkin AA, Kaloshkin SD. Low-cycle fatigue behavior of 3d-printed PLA-based porous scaffolds. *Compos Part B Eng*. 2016;97:193-200. doi:10.1016/j.compositesb.2016.04.067
48. Donate R, Monzón M, Alemán-Domínguez MEO, Ortega Z. Enzymatic degradation study of PLA-based composite scaffolds. *Rev Adv Mater Sci*. 2020;59:170-175. doi:10.1515/rams-2020-0005
49. Alemán-Domínguez ME, Ortega Z, Benítez AN, Vilarño-Feltrre G, Gómez-Tejedor JA, Vallés-Lluch A. Tunability of polycaprolactone hydrophilicity by carboxymethyl cellulose loading. *J Appl Polym Sci*. 2018;135:1-8. doi:10.1002/app.46134
50. Li S. Hydrolytic degradation characteristics of aliphatic polyesters derived from lactic and glycolic acids. *J Biomed Mater Res*. 1999;48:342-353. doi:10.1002/(SICI)1097-4636(1999)48:33.0.CO;2-7
51. Tsuji H, Ikada Y. Properties and morphology of poly(L-lactide). II. Hydrolysis in alkaline solution. *J Polym Sci Part A Polym Chem*. 1998;36:59-66. doi:10.1002/(SICI)1099-0518(19980115)36:13.0.CO;2-X
52. Nie L, Chen D, Fu J, Yang S, Hou R, Suo J. Macroporous biphasic calcium phosphate scaffolds reinforced by poly-L-lactic acid/hydroxyapatite nanocomposite coatings for bone regeneration. *Biochem Eng J*. 2015;98:29-37. doi:10.1016/J.BEJ.2015.02.026
53. Baptista R, Pereira MFC, Mauricio A, Rechená D, Infante V, Guedes M. Experimental and numerical characterization of 3D-printed scaffolds under monotonic compression with the aid of micro-CT volume reconstruction. *Bio-Design Manuf*. 2021;4:222-242. doi:10.1007/s42242-020-00122-3
54. Baptista R, Guedes M. Porosity and pore design influence on fatigue behavior of 3D printed scaffolds for trabecular bone replacement. *J Mech Behav Biomed Mater*. 2021;117:104378. doi:10.1016/j.jmbbm.2021.104378
55. Leong KF, Chua CK, Sudarmadji N, Yeong WY. Engineering functionally graded tissue engineering scaffolds. *J Mech Behav Biomed Mater*. 2008;1:140-152. doi:10.1016/j.jmbbm.2007.11.002
56. Gorrasi G, Pantani R. Hydrolysis and biodegradation of poly(lactic acid). *Adv Polym Sci*. 2018;279:119-151. doi:10.1007/12_2016_12

57. Tsuji H, Mizuno A, Ikada Y. Properties and morphology of poly(L-lactide). III. Effects of initial crystallinity on long-term in vitro hydrolysis of high molecular weight poly(L-lactide) film in phosphate-buffered solution. 2000;77. doi:[10.1002/1097-4628\(20000815\)77:73.0.CO;2-S](https://doi.org/10.1002/1097-4628(20000815)77:73.0.CO;2-S)
58. Ribeiro VP, Almeida LR, Martins AR, et al. Modulating cell adhesion to polybutylene succinate biotextile constructs for tissue engineering applications. *J Tissue Eng Regen Med.* 2017;11:2853-2863. doi:[10.1002/TERM.2189](https://doi.org/10.1002/TERM.2189)

How to cite this article: Donate R, Monzón M, Alemán-Domínguez ME, Rodríguez-Esparragón F. Effects of ceramic additives and bioactive coatings on the degradation of polylactic acid-based bone scaffolds under hydrolytic conditions. *J Biomed Mater Res.* 2022;1-13. doi:[10.1002/jbm.b.35162](https://doi.org/10.1002/jbm.b.35162)